lymphocytes. This indicates that the observed cytotoxicity depends on the integrity of the islet cell surface constituents.

Taken together, our results show that pancreatic expression of IFN-γ can result in immune sensitization of the transgenic mice to islets. In other experiments involving ectopic expression of antigens in islets, no islet immune-related destruction results, irrespective of whether tolerance is induced[9]. Indeed, there are other examples of T cells reactive to components in the periphery existing in a quiescent state[10–19]. *In vitro* experiments have demonstrated that IFN-γ can induce co-stimulatory activity leading to T cell activation[2,3], so when produced *in vivo*, it might activate quiescent autoreactive cells, stimulating lymphocytes to destroy both transgenic and normal islets. Our work implies that *in vivo* the lymphokine IFN-γ activates T cells so that they do not remain anergic to antigens encountered in the periphery. □

Received 9 April; accepted 14 June 1990.

1. Sarvetnick, N., Liggitt, D., Pitts, S. L., Hansen, S. E. & Stewart, T. A. *Cell* **52,** 773–782 (1988).
2. Hawrylowicz, C. M. & Unanue, E. R. *J. Immun.* **141,** 4083–4088 (1988).
3. Weaver, C. T., Hawrylowicz, C. M. & Unanue, E. R. *Proc. natn. Acad. Sci. U.S.A.* **85,** 8181–8185 (1988).
4. Bosma, C. G., Custer, R. P. & Bosma, M. J. *Nature* **301,** 527 (1983).
5. Duijvestijn, A. M., Schreiber, A. B. & Butcher, E. C. *Proc. natn. Acad. Sci. U.S.A.* **83,** 9114–9118 (1986).
6. Brown, J., Molnar, I. G., Clark, W. & Mullen, Y. *Science* **184,** 1377–1379 (1974).
7. Kemp, C. V., Knight, M. G., Scharp, D. W., Lacy, P. E. & Ballinger, W. F. *Nature* **244,** 447 (1973).
8. Campbell, I. L., Iscaro, A. & Harrison, L. C. *J. Immun.* **141,** 2325 (1988).
9. Harrison, L. C., Campbell, I. C., Allison, J. & Miller, J. F. A. P. *Diabetes* **38,** 815–818 (1989).
10. Mitchison, N. A. *Immunology* **15,** 509–530; 531–547 (1968).
11. Hooper, D. C., Young, J. L., Elson, C. J. & Taylor, R. B. *Cell. Immun.* **106,** 53–61 (1987).
12. Hooper, D. C. & Taylor, R. B. *Eur. J. Immun.* **17,** 797 (1987).
13. Rammensee, H. G., Kroschewski, R. & Frangoulis, B. *Nature* **339,** 541–544 (1989).
14. Qin, S., Cubbold, S., Benjamin, R. & Waldmann, H. *J. exp. Med.* **169,** 779–794 (1989).
15. Markmann, J. *et al. Nature* **336,** 476–479 (1988).
16. Burkly, L. C., Lo, D., kanagawa, O., Brinster, R. L. & Flavell, R. A. *Nature* **342,** 564–566 (1989).
17. Lo, D., Burkly, L. C., Flavell, R. A., Palmiter, R. D. & Brinster, R. L. *J. exp. Med.* **170,** 87–104 (1989).
18. Bohme, *J. et al. Science* **211,** 1179–1183 (1989).
19. Murphy, K. M., Weaver, C. T., Elish, M., Allen, P. M. & Loh, D. Y. *Proc. natn. Acad. Sci. U.S.A.* **86,** 10034–10038 (1989).

ACKNOWLEDGEMENTS. This work was supported by an MDA postdoctoral fellowship (N.S.), by a JDF postdoctoral fellowship (J.S.) and an NIH grant (J.S. and B.M.). T.G.P. is a scholar of the Leukemia Society of America. N.S. and J.S. thank Dr Garry Fathman for support.

Targeted disruption of the murine *int-1* proto-oncogene resulting in severe abnormalities in midbrain and cerebellar development

Kirk R. Thomas & Mario R. Capecchi*

Howard Hughes Medical Institute, Department of Biology and Human Genetics, Salt Lake City, Utah 84112, USA

THE *int-1* proto-oncogene was first identified as a gene activated in virally induced mouse mammary tumours[1,2]. Expression studies, however, suggest that the normal function of this gene may be in spermatogenesis and in the development of the central nervous system[3–5]. Genes sharing sequence similarity with *int-1* have been found throughout the animal kingdom. For example, *int-1* has 54% amino-acid identity to the *Drosophila* segment polarity gene *wingless* (*wg*)[6]. Both the *int-1* and *wg* gene products seem to be secreted proteins, presumably involved in cell–cell signalling[7–11]. We have now explored the function of *int-1* in the mouse by disrupting one of the two *int-1* alleles in mouse embryo-derived stem cells using positive–negative selection[12]. This cell line was used to generate a chimaeric mouse that transmitted the mutant allele to its progeny[13–16]. Mice heterozygous for the *int-1* null mutation are normal and fertile, whereas mice homozygous for the mutation may exhibit a range of phenotypes from death before birth to survival with severe ataxia. The latter pathology in mice and humans is often associated with defects in the cerebellum. Examination of *int-1*$^-$/*int-1*$^-$ mice at several stages of embryogenesis revealed severe abnormalities in the development of the mesencephalon and metencephalon indicating a prominent role for the *int-1* protein is in the induction of the mesencephalon and cerebellum.

Gene targeting has been used to disrupt numerous genes in mouse embryo-derived stem (ES) cells[12,17–28] and in several cases, germ-line transmission of the mutated gene has been reported[25–28]. The targeting vector we used to mutate *int-1*, pINT-1-N/TK, is shown in Fig. 1*a*. It contains 13 kilobases (kb) of mouse genomic DNA surrounding the *int-1* structural gene, which is interrupted in exon 2 by a 1-kb fragment containing the neomycin resistance (*neo*^{r}) gene, and flanked by copies of the thymidine kinase (*TK*) gene from herpes simplex virus.

TABLE 1 Phenotype of *int-1*$^-$/*int-1*$^-$ mice

(*a*) Mortality of *int-1*$^-$/*int-1*$^-$ mice

No. litters	No. pups	No. *int-1*$^-$/*int-1*$^-$	Day of death of *int-1*$^-$/*int-1*$^-$ pups 0–0.5	0.5–1.5	>30
5	42	10	6	3	1

(*b*) Genotype and phenotype of embryos

Days p.c.	Genotype	No. individuals	Brain morphology
14.5	+/+	3	Normal
	+/−	3	Normal
	−/−	2	Underdeveloped
17.5	+/+	7	Normal
	+/−	7	Normal
	−/−	4	Underdeveloped

Mice heterozygous at *int-1* were mated. (*a*) Mortality of live births: Five pregnancies proceeded to term and the nests examined at daily intervals. Dead offspring were removed and their DNA examined as described in the legend to Fig. 2. At day 30, DNA was extracted from tails of all living offspring and analysed by the same method. (*b*) Genotype and phenotype of embryos. Embryos were surgically removed from pregnant mothers at the times indicated and immersed in Bouin reagent. Yolk sacs were genotyped as described in Fig. 2. After 2 days in fixative, the embryonic brains were surgically removed, examined under a dissecting microscope and qualitatively compared. The 14.5-day embryos were from a single mother, the 17.5 embryos represent the sum of two pregnancies.

The *neo*^{r} gene serves both to disrupt the *int-1* protein reading frame and to provide a positive selectable marker, resistance to growth in G418, for the presence of the *int-1* mutation. The *TK* genes, lying outside *int-1* homology, function in the presence of the antiviral agent gancyclovir (GANC), as negative selectable markers that allow enrichment for cells in which homologous recombination has occurred[12].

ES cells were transformed by electroporation with the vector, pINT-1-N/TK and then grown in the presence of G418 and GANC. DNA was extracted from those colonies resistant to both drugs and analysed by Southern transfer for an insertion mutation at *int-1*. Of 5×10^8 cells surviving electroporation, 5×10^6 gave rise to G418^r colonies and 400 were resistant to both G418 and GANC. One of the G418^r-GANC^r colonies, cell-line 54, proved to contain a targeted disruption in one of the two *int-1* genes. The targeted disruption frequency for *int-1* was considerably lower than previously reported for *hprt* (ref. 17), *int-2* (ref. 12), *en-2* (ref. 20), c-*abl* (ref. 25), *IGF-II* (ref. 27) and β_2-microglobulin[22,24], which may reflect inherent differences of the loci.

* To whom correspondence should be addressed.

The demonstration of gene targeting in cell-line 54 is illustrated in Fig. 1*b*. DNAs from the parental ES cell line (CCl.2)[13] and cell-line 54 were digested with *Sac*I and analysed by Southern blotting using a hybridization probe (probe A) that contained sequences outside those found on the targeting vector. In the parental line, this probe detected a 4-kb fragment of DNA. In the mutant cell line, an additional *int-1* band of 5 kb, was evident, consistent with the insertion of the 1-kb *neo*^{r} gene into *int-1*. This interpretation was verified by digestion of this DNA with two additional restriction enzymes and probing with *neo* sequences (data not shown). The same DNAs were digested with *Bgl*II and *Xho*I and analysed with a probe (probe B) contained within the vector sequences. In addition to the wild-type allele, DNA from cell-line 54 also revealed two fragments derived from the mutant, *int-1*$^-$ allele. One of these, of 4 kb, is that predicted for the *neo*^{r} insertion; the other, of 4.3 kb, is from a tandem duplication (described in the legend to Fig. 1) and subsequent insertion of vector sequences at the target site. This duplication–insertion configuration was verified by six independent enzyme digests (data not shown) and is similar to targeting events described by others[29,30].

Chimaeric mice were generated by microinjecting the male ES cell-line 54—originally derived from a 129 Sv agouti mouse—into blastocysts from C57Bl/6 nonagouti mice. One male chimaera, when mated to a C57Bl/6 female sired pure agouti offspring indicating that his germ line contained sperm derived from ES cell-line 54. DNA prepared from tail biopsies taken from the chimaera and two of his agouti offspring was analysed by Southern transfer as shown in Fig. 2*a*. DNA from the parental ES cell line and cell-line 54 serve as controls for the *int-1*$^+$/*int-1*$^+$ and *int-1*$^-$/*int-1*$^+$ genotypes, respectively. As expected, the chimaeric father contained *int-1*$^-$ sequences, but not in stoichiometric amounts, a reflection of the degree of chimaerism in the tail. Both of his offspring, however, show the same *int-1*$^-$/*int-1*$^+$ genotype stoichiometry seen in the original mutant cell line.

The heterozygous offspring were bred with C57Bl/6 mice to establish a colony of mice heterozygous for the *int-1*$^-$ mutation. Sibling heterozygotes were mated and the pregnancies allowed to proceed to term. All offspring were genotyped at the *int-1* locus by analysing tail DNA by Southern blotting. Table 1 summarizes the fate of ten *int-1*$^-$/*int-1*$^-$ offspring (from five litters): six were dead within 0.5 days of birth; three survived 0.5 days but died before day 1.5 and one survived to adulthood. Variation in survival may reflect variation in the penetrance of the *int-1* mutation or variability in the nurturing by the mother; female mice will often separate malfunctioning offspring from the rest of the litter. But in our experiments, one out of six homozygous *int-1*$^-$ mice (two litters) examined before birth at 17.5 days p.c. died *in utero*.

The *int-1*$^-$/*int-1*$^-$ mouse that survived to adulthood was most informative regarding *int-1* function. She exhibited severe ataxia. When moving, she pivoted both clockwise and counterclockwise around her rear legs. This abnormal pattern of movement was not due to muscle wastage or defects in local motor neuron circuitry as she could jump more than 30-cm vertically. Relative to heterozygous siblings, she responded normally to stimuli of light, sound, smell and touch.

The presence of this behavioural phenotype in the *int-1*$^-$ homozygote (that is, the loss of balance and coordinated movement) suggested a defect in the cerebellum and prompted us to examine the central nervous system (CNS) in embryos produced from heterozygous matings. Embryos were removed from pregnant females at 11.5, 14.5 and 17.5 days p.c. The DNA was extracted from the yolk sacs and analysed by Southern transfer to determine the *int-1* genotype; the embryos were then fixed

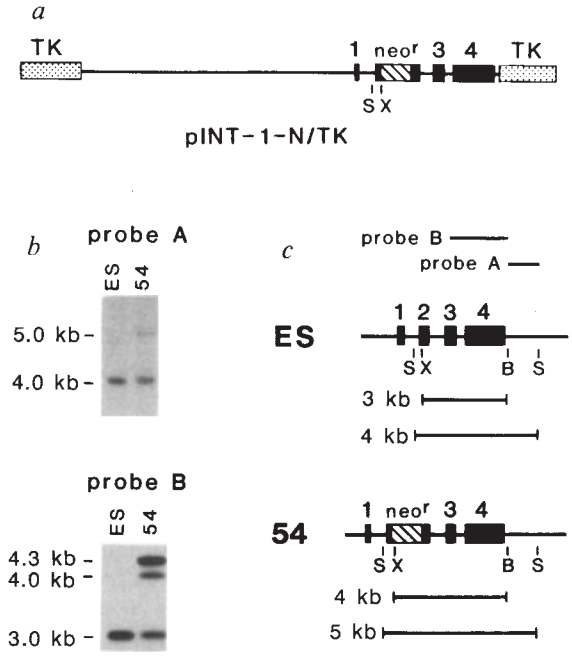

FIG. 1 *a*, The targeting vector, pINT-1-N/TK, consists of 13.5 kb of mouse genomic sequences, containing the *int-1* gene interrupted at the *Xho*I site in exon 2 (ref. 2) with the *neo*^{r} gene from pMCI-Neo (ref. 17). The *int-1-neo*^{r} sequences are flanked by copies of the *HSV-TK* gene from pMCI-TK (ref. 12). Narrow lines, introns; black boxes, exons; hatched boxes, *neo*^{r}; stippled boxes, *HSV-TK*. The vector was linearized by digestion with *Sal*I, and introduced into ES cell line CC1.2 by electroporation. Aliquots of cells were subjected to three growth conditions: non-selective medium to assess viability (50% of the starting cells survived electroporation); G418 medium to assay the fraction of cells stably transformed by the vector; and G418 plus GANC medium to enrich for transformants containing a *neo*^{r} insertion at one of the *int-1* loci. DNA from cells surviving G418-GANC selection were subjected to Southern transfer analysis as shown in *b*. Note: The presence of flanking *TK* sequences was included to add an additional enrichment to the positive–negative selection protocol. Previous data suggested that a large fraction of non-targeted, yet GANC^r, cells transformed with vector containing a single *TK* survived because of transfection-induced alterations of the *TK* gene[12]. The presence of the second copy of the *TK* sequences does seem to enhance the enrichment factor from the 10^3 seen previously, to 10^4 (that is, $5\times10^6/4\times10^2$), seen in Table 1. We have shown that blocking none, one, or both ends of a targeting vector has no detectable effect on the frequency of homologous recombination at the *hprt* locus (K.R.T. and M.R.C., unpublished observations). *b*, Identification of an *int-1*$^+$/*int-1*$^-$ cell line. ES, DNA from cell line CC1.2, 54, DNA from the G418^r, GANC^r cell line transfected with pINT-1-N/TK. Sizes of the bands are indicated (kb). DNAs hybridized to probe A were digested with *Sac*I; those to probe B with *Bgl*II and *Xho*I. The *int-1*$^+$ allele gives a stronger signal than the *int-1*$^-$ allele because of wild-type sequences in the feeder cells used to propagate the ES cells. *c*, A schematic representation of the Southern transfer data. ES is a map of the wild-type *int-1*$^+$ locus; 54 is a map of the *int-1*$^-$ allele containing a *neo*^{r} insertion in exon 2. Beneath each gene are shown the positions of diagnostic restriction endonuclease cleavage sites, and the length of the digestion products. Positions of the probes are indicated above the maps. Probe A (DNA sequence not present in the targeting vector) is a 1-kb *Bgl*II–*Hind*III fragment 3′ of the *int-1* gene (gift of R. Nusse); Probe B is a 2-kb *Cla*I–*Bam*HI fragment within the *int-1* gene. B, *Bgl*II; S, *Sac*I; X, *Xho*I. When DNA from cell line 54 is hybridized with probe B, which consists of sequences from within the vector pINT-1-N/TK, an unexpected fragment 4.3 kb in length is seen. This fragment represents additional copies of the vector sequences that have integrated in a tandem array 5′ to those sequences depicted. Such a configuration is most likely the result of the head-to-tail concatamerization of the vector before its recombination with the target locus. The 4.3-kb fragment extends from the *Xho*I site in exon 2 to a *Bgl*II site in the targeting vector and is predicted from the map of the vector. Digestions of DNA from cell-line 54 with six additional restriction endonucleases and hybridization with *neo*^{r} probes verify this configuration. The above analysis also showed that DNA sequences both 5′ and 3′ to the *int-1* locus were not altered, demonstrating that the targeted mutation was limited to the *int-1* gene.

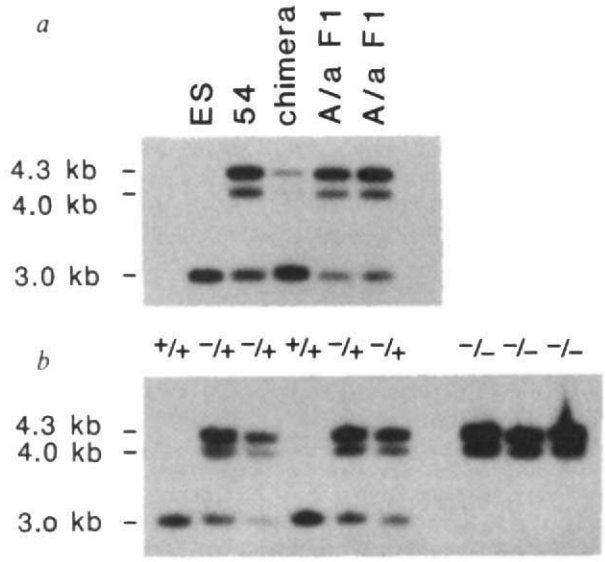

FIG. 2 Transmission of the *int-1*$^-$ genotype. *a*, Cell lines and founding animals. ES cell line 54 was microinjected into 4.5 day C57Bl/6 preimplantation embryos, surgically transferred into the uterus of pseudopregnant mice and allowed to come to term. Two resulting male chimaeras were test bred with C57Bl/6 females for transmission of agouti offspring. One of these males proved to be a germ-line chimaera. DNA was extracted from cell lines (ES and 54) or from tail biopsies, digested with *Xho*I and *Bgl*II, and analysed with probe B as described in the legend to Fig. 1. ES, the parental cell line CC1.2; 54, the *int-1*$^+$/*int-1*$^-$ cell line carrying the targeted mutation in *int-1*. Chimaera designates the founding chimaeric male; A/a and A/a are his agouti offspring produced following mating with a C57Bl/6 female. *b*, Transmission to embryos. Heterozygous offspring from A/a and A/a shown in *a* were mated. Following 17.5 days gestation, the embryos were removed from the mother. DNA was extracted from the yolk sac surrounding each individual embryo and analysed by Southern transfer as described in Fig. 1. The genotype at *int-1* is indicated above each lane: +, wild type; −, *neo*^{r} insertion in exon 2.

and dissected. DNA analyses of nine embryos from one pregnancy is illustrated in Fig. 2*b* and all three expected genotypes were clearly present. The results of visual analyses of the fetal brains are summarized in Table 1(*b*). After 11.5 days of gestation, morphological differences between heterozygous and homozygous *int-1*$^-$ mice were not readily apparent. But by 14.5 days, malformations in the mesencephalon and metencephalon were apparent. At 17.5 days, this malformation was translated into mild midbrain hydrocephaly. This malformation was 100% concordant with the homozygous *int-1*$^-$ genotype: 6/6 embryos of *int-1*$^-$/*int-1*$^-$ genotype exhibited this phenotype, whereas 20/20 *int-1*$^+$/*int-1*$^+$ and *int-1*$^+$/*int-1*$^-$ embryos showed normal brain development. Figure 3*a* and *b* compares dorsal views of brains from *int-1*$^-$/*int-1*$^+$ and *int-1*$^-$/*int-1*$^-$ embryos at 17.5 days of gestation. It is apparent from macroscopic examination alone, that the mesencephalon and metencephalon are highly defective. This is corroborated by examination of sagittal and parasagittal sections of the same brains (Fig. 3*c*, *d*). In the *int-1*$^-$ homozygote, the cerebellum and a large portion of the mesencephalon, as indicated by the arrows, are not visible. As a reference point, note that the posterior choroid plexus (pcp) is present in both brains. The embryos used for the above analysis, from the same mating, showed normal embryonic leg and head movement and touch response. The telencephalon as judged from examination of both parasagittal and coronal sections, appeared to be normal. However, in the *int-1*$^-$ homozygous mouse, the frontal lobes of the brain do seem to extend more caudally relative to the heterozygous mate, perhaps a result of expansion into regions normally occupied by the missing parts of the midbrain.

The *int-1*$^-$/*int-1*$^-$ mouse that survived until adulthood exhibited hydrocephally in the caudal region of the cerebral hemispheres as well as in the midbrain. Examination of sagittal and parasagittal sections of this *int-1*$^-$/*int-1*$^-$ brain corroborated the presence of the hydrocephally but also unexpectedly showed that the posterior portion of the cerebellum was present (Fig. 3*e*, *f*). In this context, it is interesting that Wilkinson *et al.*[5] did not observe *int-1* messenger RNA in the 10.5-day rostral hindbrain. Furthermore, LeDouarin and co-workers have recently provided evidence that in the chick, the anterior portion of the cerebellum may be derived from the mesencephalon, whereas the posterior portion comes from the metencephalon[31]. If this is also true for the mouse, then the phenotypic influence of the *int-1* mutation in this mouse may have respected the mesencephalon–metencephalon boundary.

In summary, heterozygous *int-1*$^-$ mice seem normal. A prominent effect of disrupting both *int-1* alleles is a major defect in the development of the midbrain and cerebellum. In fact, it seems that *int-1* protein is required in the induction of a large portion of the mesencephalon and of the cerebellum as in its absence these structures are not formed normally. Further, the *int-1* homozygote that survived to adulthood displayed the classical, although a more extreme, form of symptomatology attributed to human and mouse cerebellar defects (that is, severe ataxia).

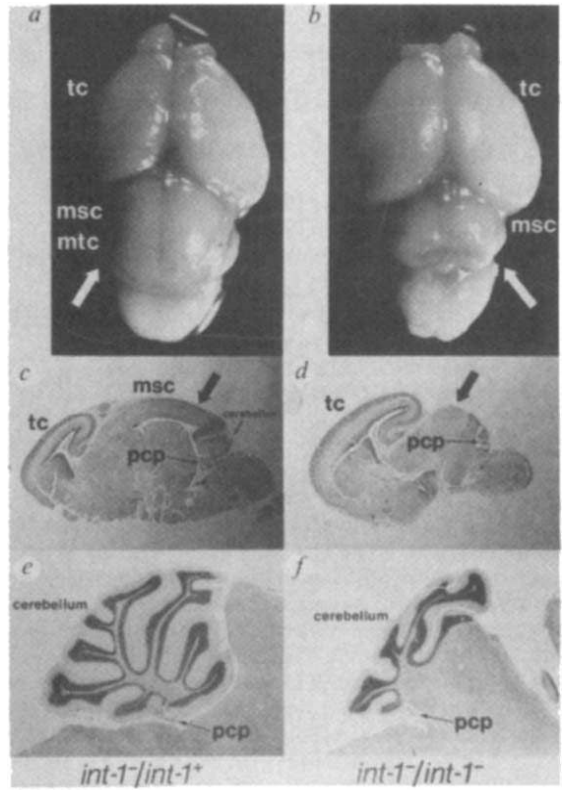

FIG. 3 Comparison of brains from heterozygous and homozygous, *int-1*$^-$ mice. *a*, and *b*, 17.5 day embryos were fixed in Bouin's reagent (Sigma). The yolk sacs were removed for DNA analysis as described in Table 1. Following two days in fixative, the brains were dissected, rinsed in PBS and photographed at ×6 magnification. The field of view is 5×10 mm. Arrows indicate the cerebellar region absent in the homozygote. *c* and *d*, The brains shown in *a* and *b* were embedded in paraffin, sectioned (10 μm), and stained by haematoxylin and eosin (H and E) regressive staining. The field of view is 6×4 mm. Arrows indicate mesencephalic tissue absent in the homozygote. *e* and *f*, Brains were dissected from adult (5 week) mice, fixed in PLP, embedded in paraffin, sectioned (8 μm) stained with H and E. The field of view is 6×4 mm. tc, telencephalon; msc, mesencephalon; mtc, metencephalon; pcp, posterior choroid plexus.

In the 17.5-day embryo, cellular structures corresponding to the cerebellum are not observed. But in the mouse that survived to adulthood, the posterior portion of the cerebellum was present. An intriguing hypothesis to explain this difference is that the dependency on the inductive influence of *int-1* exhibits a rostral–caudal gradient beginning in the mesencephalon and spreading to the metencephalon. This could produce differences in the penetrance of the *int-1*$^-$ mutation such that some mice lack only the anterior portion of the cerebellum, whereas others are missing the entire cerebellum.

The *int-1* gene is expressed during the ontogeny of the CNS along the dorsal midline of the developing neural tube from the midbrain to the tail[5]. From analysis of sagittal and transverse sections, in either embryos or in the *int-1*$^-$ survivor, we have not observed morphological defects in the spinal cord. This may indicate that either *int-1* expression in this region of the developing CNS is spurious or that another gene, perhaps another member of the *int-1* family, can substitute for *int-1* function in the development of the spinal cord. □

Received 20 July; accepted 6 August 1990.

1. Nusse, R. & Varmus, H. E. *Cell* **31,** 99-109 (1982).
2. van Ooyen, A. & Nusse, R. *Cell* **39,** 233-240 (1984).
3. Jakobovits, A., Shackleford, G. M., Varmus, H. E. & Martin, G. R. *Proc. natn. Acad. Sci. U.S.A.* **83,** 7806-7810 (1986).
4. Shackleford, G. M. & Varmus, H. E. *Cell* **50,** 89-95 (1987).
5. Wilkinson, D. G., Bailes, J. A. & McMahon, A. P. *Cell* **50,** 79-88 (1987).
6. Rijsewijk, F. *et al. Cell* **50,** 649-657 (1987).
7. Morata, G. & Lawrence, P. A. *Devl Biol.* **56,** 227-240 (1977).
8. Baker, N. E. *EMBO J.* **6,** 1765-1770 (1987).
9. Papkoff, J., Brown, A. M. C. & Varmus, H. E. *Molec. cell. Biol.* **7,** 3978-3984 (1987).
10. Bradley, R. S. & Brown, A. M. *EMBO J.* **9,** 1569-1575 (1990).
11. Papkoff, J. & Schryver, B. *Molec. cell. Biol.* **10,** 2723-2730 (1990).
12. Mansour, S. L., Thomas, K. R. & Capecchi, M. R. *Nature* **336,** 348-352 (1988).
13. Bradley, A., Evans, M., Kaufman, M. H. & Robertson, E. *Nature* **309,** 255-256 (1984).
14. Capecchi, M. R. *Trends Genet.* **5,** 70-76 (1989).
15. Capecchi, M. R. *Science* **244,** 1288-1292 (1989).
16. Rossant, J. & Joyner, A. *Trends Genet.* **5,** 277-283 (1989).
17. Thomas, K. R. & Capecchi, M. R. *Cell* **51,** 503-512 (1987).
18. Doetschman, T., Maeda, N. & Smithies, O. *Proc. natn. Acad. Sci. U.S.A.* **85,** 8583-8587 (1988).
19. Zimmer, A. & Gruss, P. *Nature* **338,** 150-153 (1989).
20. Joyner, A. L., Skarnes, W. C. & Rossant, J. *Nature* **338,** 153-156 (1989).
21. Johnson, R. S. *et al. Science* **245,** 1234-1236 (1989).
22. Koller, B. H. & Smithies, O. *Proc. natn. Acad. Sci. U.S.A.* **86,** 8932-8935 (1989).
23. Mansour, S. L., Thomas, K. R., Deng, C. & Capecchi, M. R. *Proc. natn. Acad. Sci. U.S.A.* (in the press).
24. Zijlstra, M., Li, E., Sajjadi, F., Subramani, S. & Jaenisch, R. *Nature* **342,** 435-438 (1989).
25. Schwartzberg, P. L., Goff, S. P. & Robertson, E. J. *Science* **246,** 799-803 (1989).
26. Zijlstra, M. *et al. Nature* **344,** 742-746 (1990).
27. DeChiara, T. M., Efstratiadis, A. & Robertson, E. J. *Nature* **345,** 78-80 (1990).
28. Koller, B. H., Marrack, P., Kappler, J. W. & Smithies, O. *Science* **248,** 1227-1230 (1990).
29. Fell, H. P., Yarnold, S., Hellstrom, I., Hellstrom, K. E. & Folger, K. R. *Proc. natn. Acad. Sci. U.S.A.* **86,** 8507-8511 (1989).
30. Schwartzberg, P. L., Robertson, E. J. & Goff, S. P. *Proc. natn. Acad. Sci. U.S.A.* **87,** 3210-3214 (1990).
31. Hallonet, M. R., Teillet, M. & LeDouarin, N. M. *Development* **108,** 19-31 (1990).

ACKNOWLEDGEMENTS: We thank S. Tamowski, C. Lenz, M. Allen and E. Nakashima for technical assistance, T. Musci and R. Mullen for assistance and advice on histology, R. Nusse for providing the *int-1* flanking probe, D. Gard and F. Brown for help with photography.

'Formins': proteins deduced from the alternative transcripts of the *limb deformity* gene

Richard P. Woychik*, Richard L. Maas*, Rolf Zeller*, Thomas F. Vogt & Philip Leder

Department of Genetics, Harvard Medical School, and Howard Hughes Medical Institute, 25 Shattuck Street, Boston, Massachusetts 02115, USA

VERTEBRATE limb formation is an evolutionarily conserved process programmed by an array of morphogenetic genes[1–5]. As a result of transgene insertion, we previously identified a mutation at the mouse limb deformity (*ld*) locus that disrupts embryonic pattern formation, resulting in a reduction and fusion of the distal bones and digits of all limbs as well as variable incidence of renal aplasia[2,6–9]. We have now characterized the *ld* locus at the molecular level. It contains evolutionarily conserved coding sequences that are transcribed in adult and embryonic tissues as a complex group of low abundance messenger RNAs created by alternative splicing and differential polyadenylation. The association of these transcripts with the gene responsible for the mutant phenotype was established by demonstrating that they are disrupted in two independently arising *ld* alleles[8]. We have now deduced the structure of several novel proteins (termed formins) from the long open reading frames encoded by the various *ld* transcripts. The observation of these different RNA transcripts in different tissues suggests that the formins play a part in the formation of several organ systems.

A map of both the mutant and wild-type loci is shown in Fig. 1*a*. Insertion of the transgene into the (*ld*) locus was accompanied by deletion of about 1.5 kilobases (kb) of endogenous genomic DNA[6]. No other rearrangements were observed. We first identified potential exons along the genomic DNA by searching for evolutionarily conserved regions. Two of these appeared as likely coding exons because, when sequenced, they revealed short open reading frames flanked by splice acceptor–donor sequences (A and B in Fig. 1*a*). Cross-hybridizing regions were cloned from human and chicken genomic libraries and examined for sequence homology. The nucleotide sequences of regions A and B are 80–90% conserved between humans and mice. For example, the extent of sequence conservation of one putative exon (Fig. 1*a*, region B) is shown by comparing the homology regions of the mouse, human and chicken genomes (Fig. 1*b*).

Complementary DNA libraries prepared from RNA isolated from adult kidney and testis (two organs in which transcripts were most abundant) yielded overlapping cDNA clones that were identified using a genomic DNA probe containing the evolutionarily conserved exon B (shown in Fig. 1*a*, *b*). Sequence analysis of these cDNAs, illustrated by ten representative cDNA clones (Fig. 2), demonstrates a complex pattern of mRNA synthesis (see also Fig. 3). These cDNAs reveal differential use of polyA addition sites separated by several kilobases as well as alternative splicing of internal (see clones 2, 3, 4, 5, 7 and 9, Fig. 2) and 5′ exons (see clone 1, Fig. 2). Long, but variably composed open reading frames (ORFs) (see below) were deduced from nucleotide sequence analysis.

The complexity of the RNA products of the *ld* locus is reflected by the various transcripts observed in analyses of RNA from both embryonic and adult tissues (Fig. 3). A transcript important in morphogenesis of limb and kidney should be present before or at the time of the morphological observation of the mutant phenotype. Expression of the *ld* gene as assayed by RNase protection occurs in primitive-streak embryos (gestational day seven) before limb development[9]. To examine the pattern of RNA transcripts in the embryo, RNA was isolated from gestational day 9–12 embryos and analysed as shown in Fig. 3*a*. Three main classes of mRNAs (~13, 7 and 3 kb) are detected in all parts of the embyro (Fig. 3*a*) including the limb buds. The size differences observed between these transcripts result from differential utilization of the three sets of poly(A)

* Present addresses: Biology Division, Oak Ridge National Laboratories, PO Box 2009, Oak Ridge, Tennessee 37831, USA (R.P.W.), Department of Medicine, Brigham & Women's Hospital, Howard Hughes Medical Institute, Boston, Massachusetts 02115, USA (R.L.M.), and EMBL, Postfach 10.2209, Meyerhofstr. 1, D-6900 Heidelberg, FRG (R.Z.).